Journal of Digital Imaging (2018) 31:718–726
https://doi.org/10.1007/s10278-018-0063-1

# Deformable Registration for Longitudinal Breast MRI Screening

Hatef Mehrabian[1] · Lara Richmond[2] · Yingli Lu[1] · Anne L. Martel[1,3]

Published online: 13 April 2018


**Abstract**
MRI screening of high-risk patients for breast cancer provides very high sensitivity, but with a high recall rate and negative biopsies. Comparing the current exam to prior exams reduces the number of follow-up procedures requested by radiologists. Such comparison, however, can be challenging due to the highly deformable nature of breast tissues. Automated co-registration of multiple scans has the potential to aid diagnosis by providing 3D images for side-by-side comparison and also for use in CAD systems. Although many deformable registration techniques exist, they generally have a large number of parameters that need to be optimized and validated for each new application. Here, we propose a framework for such optimization and also identify the optimal input parameter set for registration of 3D $T_1$-weighted MRI of breast using Elastix, a widely used and freely available registration tool. A numerical simulation study was first conducted to model the breast tissue and its deformation through finite element (FE) modeling. This model generated the ground truth for evaluating the registration accuracy by providing the deformation of each voxel in the breast volume. An exhaustive search was performed over various values of 7 registration parameters (4050 different combinations of parameters were assessed) and the optimum parameter set was determined. This study showed that there was a large variation in the registration accuracy of different parameter sets ranging from 0.29 mm to 2.50 mm in median registration error and 3.71 mm to 8.90 mm in 95 percentile of the registration error. Mean registration errors of 0.32 mm, 0.29 mm, and 0.30 mm and 95 percentile errors of 3.71 mm, 5.02 mm, and 4.70 mm were obtained by the three best parameter sets. The optimal parameter set was applied to consecutive breast MRI scans of 13 patients. A radiologist identified 113 landmark pairs (~ 11 per patient) which were used to assess registration accuracy. The results demonstrated that using the optimal registration parameter set, a registration accuracy (in mm) of 3.4 [1.8 6.8] was achieved.

**Keywords** Breast MRI · Non-rigid registration · Finite element analysis · Elastix

## Introduction

Dynamic contrast-enhanced (DCE)-MRI has been shown to have high sensitivity in breast cancer detection [1–3]. Tumors can appear as bright enhancing masses in the DCE-MRI images. The radiologist evaluates the pattern of mass enhancement and washout of contrast agent from the mass over time. Malignant tumors tend to demonstrate a rapid signal enhancement followed by a rapid washout [4] while benign ones generally demonstrate continued increase in signal over time [3]. In clinical breast cancer screening, a high-resolution pre-contrast volume is acquired and then approximately four series are acquired following an injection of a contrast agent, generally separated by approximately 2-min intervals [5, 6]. Fat suppression and/or image subtraction is used to highlight the contrast-enhancing regions and the radiologist will assess the shape, margins, and the enhancement characteristics of the lesion [7] in order to determine whether the lesion is likely to be malignant or benign.

When interpreting images, radiologists will also make use of previous MRI studies, if they are available. A new or rapidly growing lesion is more likely to be a malignant tumor as compared to a lesion that changes very slowly [8]. Other suspicious changes can include a change in the shape or enhancement characteristics of the lesion. It has been reported that patients are significantly less likely to be referred to a short-interval follow-up if a previous baseline study is available for comparison [9] and a similar result was reported previously in

✉ Hatef Mehrabian
hatef.mehrabian@sunnybrook.ca

[1] Physical Sciences, Sunnybrook Research Institute, 2075 Bayview Ave, Toronto, ON M4N 3M5, Canada

[2] Department of Medical Imaging, Sunnybrook Health Sciences Centre, Toronto, ON, Canada

[3] Department of Medical Biophysics, University of Toronto, Toronto, ON, Canada

mammography [10]. In order to make a visual comparison of two breast MRI datasets, the radiologist typically makes use of landmarks such as blood vessels [11] to identify corresponding slices. If, however, differences in positioning during image acquisition lead to deformation of the breast, it may be difficult to establish a visual correspondence between the two exams and it can be challenging to determine whether a lesion was present on a previous scan or whether its appearance has changed. There exist very few studies that have evaluated co-registration accuracy between multiple visits of patients, highlighting the need for such investigations [12].

There has been a large body of work in medical image registration in the past decades. A comprehensive overview of the work done to date is provided by Oliveira et al. [13]. Viergever et al. [14] also provided a review of the advances that have taken place in the past 20 years. This paper highlighted the need for validation techniques for accessing the accuracy of image registration techniques which is the main obstacle in their clinical adaptation. There exist several registration tools that can be used for non-rigid registration of breast volumes. Our group has developed a fast deformable registration method that is based on optical flow [15], but this method was designed for motion correction during a single exam and cannot reliably correct for the large deformations which occur when repositioning the patient between visits. There have also been several studies evaluating the performance of different registration algorithms which conclude that deformable registration is required for breast registration even in case of registering the multiple time points of the same visit [16, 17]. These studies aimed at removing motion artifacts resulting from breathing and also slight movements of the patient during the DCE-MRI scan of the breast. The deformations in these cases are significantly smaller than multiple visits of the patient which result from different positionings of the patient, differences in the applied forces to fix the breast during the scan, as well as changes that might occur in breast volume due to weight loss/gain, etc.

Co-registration of breast MRI between multiple scans, despite being similar to the motion artifact during a DCE-MRI scan [16, 17], is a fundamentally different problem that needs to be investigated and the optimal setting for such registration needs to be identified. The main challenge in the former is large deformations and change in shape, whereas in the latter, is changes in image contrast due to administration of contrast agent. The most widely used open-source registration tools are Elastix [18] and ANTS [19]. In this study, we will focus on Elastix since the ANT toolkit is very slow and for the case of a typical breast MRI (512 × 512 × 30 voxels), it takes more than 1 h to obtain an accurate registration (on a regular computer). Elastix, on the other hand, is capable of performing such registration in 3–5 min.

Every deformable registration algorithm has numerous parameters that have to be tuned. Selecting an inappropriate parameter set results in inaccurate registration with large errors. For a specific application, it is of utmost importance to determine the parameter set that provides the optimal registration accuracy. The goal of this study was to develop a framework for determining the optimal parameters which could be applied to any similar problem. We apply this framework to registration of breast MRI between multiple visits of a patient. In this framework, we first simulate the breast tissue deformation through finite element analysis using the mechanical properties of the breast tissues, and then apply a realistic mechanical deformation to this numerical model. This model provides the ground truth for the deformation that each voxel in the breast volume undergoes between the two scans. Then, we perform an exhaustive search of registration parameters to determine the optimal set for breast MRI registration. In order to evaluate the performance of this framework, we apply the optimal parameter set to patient data and use anatomical landmarks, identified by a radiologist, to evaluate accuracy.

## Methods

### Numerical Study

A numerical simulation study was conducted to simulate deformation of breast tissue between MRI scans at two consecutive visits. A mechanical model of the breast tissue was constructed using finite element (FE) analysis [20–22]. The objective of this numerical study was to develop a realistic deformation model that could be used in evaluating registration accuracy and optimizing parameters.

The breast FE model was comprised of adipose and fibroglandular tissues and each tissue type was assigned its appropriate mechanical properties as reported in the literature [22]. In order for the model to contain a realistic distribution of fat and fibroglandular tissue, a 3D $T_1$-weighted MRI volume of a patient (without fat saturation) was used. This breast MRI was acquired with a 1.5 T GE Signa (GE Healthcare, Waukesha, WI) with sagittal orientation, 0.49 $mm^2$ in plane resolution, and 3 mm slice thickness. At this step, a breast volume without a tumor was used since our goal was to determine the optimal parameter set for breast screening, where most exams will either be normal or will only show a small tumor. The breast volume was first segmented to remove the chest wall and then a threshold value was used to separate the two tissue types and generate masks of each tissue. Figure 1 shows a cross section of this $T_1$-weighted MRI dataset (after segmentation of the breast volume) which shows the fibroglandular tissue with low intensity and fat with high-intensity voxels.

Once the voxels corresponding to each tissue type were identified, a 3D mesh was generated for the model using 3D triangular elements (ABAQUS element type C3D6H) such that each voxel was assumed to be comprised of 2 elements and the

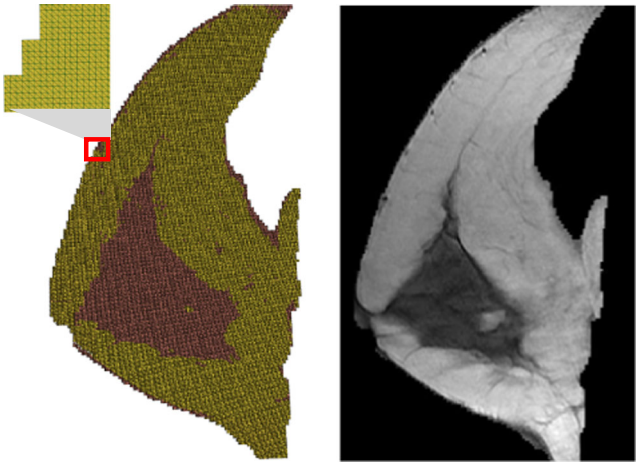

**Fig. 1** Right: A representative slice of the $T_1$-weighted MRI volume of one patients showing the fat and fibroglandular tissues. Left: The mesh that was generated from the MRI data and was used in finite element analysis. Each MRI voxel (square shape) was represented by 2 triangular elements in the mesh as can be seen in the zoomed in segment of the image. The voxels corresponding to the two tissue types in the breast are depicted with different colors. This separation was determined by dividing the voxels into two groups with a threshold in MRI signal intensity (fat appears with high intensity and fibroglandular tissue has low intensity in $T_1$-weighted MRI without fat suppression). The elements corresponding to fat are shown in yellow and the elements corresponding to fibroglandular tissue are shown in red

physical coordinates of the apexes of the voxel were used as the nodes of the mesh. Thus, each MRI voxel was represented by 2 elements and 8 nodes. Poison's ratio of 0.495 was assumed for the elements to ensure incompressibility of the tissue [23]. A cross section of this mesh is also shown in Fig. 1 (with the two tissue types being represented with different colors).

In order to apply a realistic deformation to our model, we used the MRI data of the patient at two visits and applied the Elastix registration - with an arbitrary set of parameters - to the surfaces of the two datasets. The resultant deformation field of the surface of the breast at visit one was then used as prescribed displacement boundary condition in our FE model which was consequently simulated using the commercial ABAQUS finite element analysis software. Note that using Elastix to estimate the surface deformation does not affect the generality of our approach. This step was only used to obtain a sense of the deformations that a typical breast undergoes. However, the actual deformation of each voxel was simulated by applying the mechanical model and was determined by the FE model. Table 1 reports the details of the FE model that was used in this study.

## Elastix Registration

We focused on the B-spline-based non-rigid registration as implemented by Elastix [18] which is a widely used and freely available registration package. B-splines are piecewise polynomial-based smooth functions of minimum support

**Table 1** Parameters used in the numerical finite element (FE) model of breast tissue

| Parameter | Value |
|---|---|
| Young's modulus (fat) | 3.25 kPa |
| Young's modulus (fibroglandular tissue) | 3.20 kPa |
| Poison's ratio | 0.495 |
| Element dimensions | $3 \times 0.49 \times 0.49$ |
| Element type | C3D6H |
| Number of elements | 1,379,324 |
| Number of slices | 20 |

(i.e., other spline types can be expressed in terms of B-splines) and have been previously used in non-linear registration of highly deformable cases of breast MRI [24]. This registration algorithm has a large number of parameters that need to be tuned for any given problem. We attempted to determine the optimal parameter set for Elastix that provided the highest accuracy in co-registering 3D $T_1$-weighted MRI of the breast (without fat suppression), which is the most commonly used modality by the radiologists in breast MRI screening. Affine transformation was also used for rigid registration prior to applying the B-spline-based deformable registration using mutual information as the similarity metric.

The similarity metric for intensity-based registration used throughout this study was mutual information [25] which is known as the "AdvancedMattesMutualInformation" in Elastix. Table 2 lists all the parameters that were investigated in the deformable registration and the ranges that were studied. If a single value is reported for a parameter, the value of that parameter was fixed in all analyses. For the simulation study, an exhaustive search was performed on all different combinations of these parameters (4050 combinations in total) and the optimal parameter set was determined.

## Patient Study

In order to evaluate the performance of the registration and the selected parameters in clinical cases, a total of 13 patients (5 patients with malignant tumors, 4 patients with benign tumors, and 4 patients without a lesion) were MRI-scanned twice with the clinically used sequences under a research ethics board (REB) approved protocol. The $T_1$-weighted MRI (without fat suppression) that were used in this study were acquired on a 1.5 T GE Signa (GE Healthcare,Waukesha, WI) with sagittal orientation, 0.49 $mm^2$ in plane resolution, and 3 mm slice thickness. The patients were MRI-scanned in prone position and the level of breast compression could vary between visits. This study focused on the pre-contrast phase of the imaging that did not involve contrast agent injection.

An expert radiologist (with 7 years of experience in reading breast MRI) identified 8–11 structural landmarks (113

**Table 2** All the parameters used in non-rigid registration with Elastix

| Parameter | Values |
|---|---|
| NumberOfSpatialSamples | 4096 |
| FinalGridSpacingInPhysicalUnits | 4, 8, 16, 24, 32 |
| Transform | BSplineTransform |
| NumberOfResolutions | 2, 3, 4 |
| Optimizer | AdaptiveStochasticGradientDescent |
| MovingImagePyramid | MovingRecursiveImagePyramid |
| NumberOfHistogramBins | 32, 64 |
| Interpolator | BSplineInterpolator |
| ResampleInterpolator | FinalBSplineInterpolator |
| MaximumNumberOfIterations | 100, 300, 500, 1000 |
| BSplineInterpolationOrder | 2, 3, 4 |
| FixedImagePyramid | FixedRecursiveImagePyramid |
| Metric (similarity for non-rigid registration) | AdvancedMattesMutualInformation |
| TransformRigidityPenalty | 0, 0.1, 0.2, 0.3, 0.5 |
| Registration | MultiMetricMultiResolutionRegistration |
| FinalBSplineInterpolationOrder | 2, 3, 4 |

landmarks in total) in the two scans of each patient which were used for assessing the accuracy of the registration. The ClearCanvas viewer (Synaptive Medical, Toronto, ON, Canada) was adapted to allow for annotating the images. The landmarks were identified at various slices on the 3D breast volume and included blood vessels, nipple, specific combinations of the fibroglandular tissue, and adipose tissue, e.g., a narrow band of fibrogralduldar tissue extending into the adipose, certain edge structures of the fibroglandular tissue, etc. A sample slice of one of the patient datasets at visit one and its corresponding slice (having the same physical coordinate) at visit two (before and after registration) are shown in Fig. 2. The radiologist's landmarks are also shown with the arrows which, as can be seen in Fig. 2a, c, correspond to the same anatomical structure but do not lay at the same coordinate (the boxes in these images have the same physical coordinate). Thus, co-registration is needed to align the two breast volumes. As can be seen in Fig. 2e, Elastix registration resulted in accurate alignment of the two volumes.

## Data Analysis

In order to determine the parameter combination with the optimal registration accuracy, the following parameters of the deformable registration were varied (within the ranges specified in Table 2): number of resolution levels, number of iterations, number of histogram bins when calculating mutual information, transform rigidity penalty which penalizes the non-rigid deformation by penalizing the bending on the voxel grid to avoid unrealistic deformations, and final grid spacing which specifies the control point lattice spacing in the grid for calculating the B-splines, as well as the B-spline interpolation order and the final B-spline interpolation order.

In case of the simulation study, the registration accuracy was evaluated by measuring the Euclidian distance (in mm) between the location of each voxel determined from the FE analysis and its corresponding location in the registered volume. There were a large number of voxels in each breast (in the order of 10^5) and the error in most voxels was relatively small, which resulted in the distribution of the voxel registration errors being positively skewed; therefore, the median, interquartile range, and 95 percentile values of the error distribution were used as the summary statistic. In order to determine if the median registration accuracies were different as parameter values were being changed, the Wilcoxon rank-sum test (which is a non-parametric test), was used. The statistical significance level was set at $p < 0.05$.

Similarly, for the patient study, we report the median value of the registration error. However, having a small number of points, we report the 25 and 75 percentile range, rather than the 95 percentile that was reported in the numerical simulation study. All the analysis was performed on a 64 bit PC with Windows 7 operating system, Intel Core i5 CPU (3.33 GHz) with 16 GB of RAM without using any GPU acceleration and the Elastix version 4.7 was used.

## Results

The exhaustive search was first performed on the numerical breast model to determine the optimal parameter set. A total of 4050 registrations were performed and the registration accuracy was calculated for each run. The duration of each registration was also recorded.

Figure 3 shows the distribution of the median registration error for different values of each parameter. For each boxplot

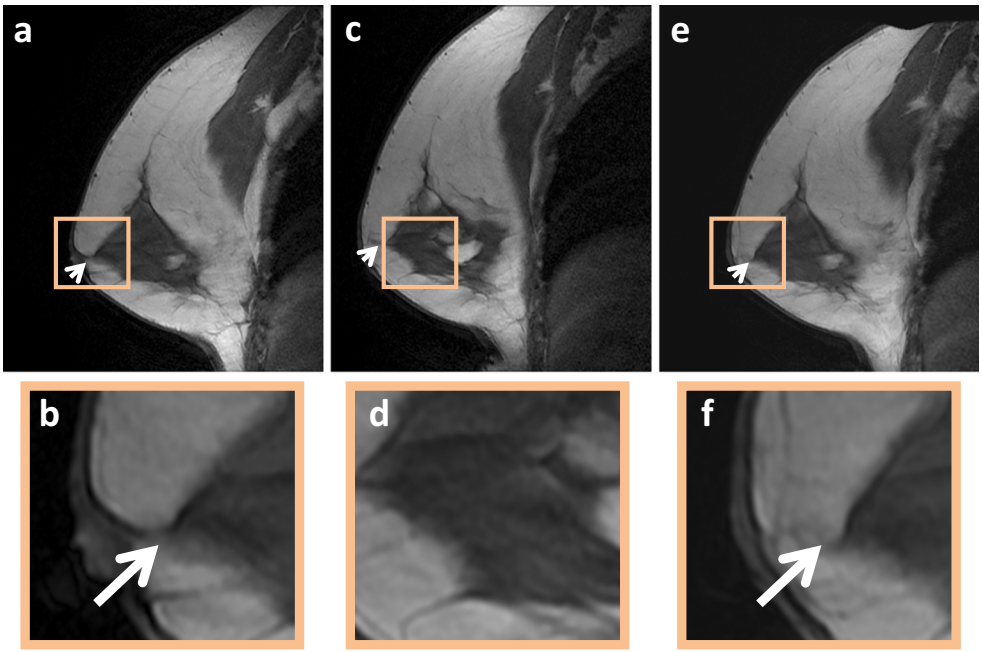


**Fig. 2** A representative slice of the 3D $T_1$-weighted MRI of a patient at two visits (**a** and **c**) as well as the corresponding co-registered image (**e**) resulting from co-registering the 3D volume of the image in (**c**) to the 3D volume of the image in (**a**). In sub-figures (**b**), (**d**), and (**f**), the portion of the full image inside the orange box is enlarged for better visualization. The arrows show the anatomical landmarks that the radiologist had identified in the two data sets (in (**d**), the landmark falls outside of the orange box). These landmarks were used to evaluate the performance of the registration algorithm

in Fig. 3, a single parameter is kept constant and all different combinations of the remaining parameters are explored. The Wilcoxon rank-sum test was used to determine the difference between these distributions which demonstrated that only the "Final Grid Spacing in Physical Units" had a statistically significant effect on the registration error. In the other plots, the distribution of the median errors were similar. Thus, the intra-class variations dominate the inter-class variations in registration errors which shows that no single parameter can be tuned independently and that the parameter combinations should be considered.

In Fig. 4, the plots show the median and 95 percentile registration error for a down-sampled version of the search domain. Given the large number of parameter combinations, the parameter sets that provided mean registration errors that were less than 0.01 mm different are shown with only one point (for better visualization). It can be seen in this figure that there was no pattern in the distribution of registration errors and that there were several parameter sets that provided very high registration accuracies (median error < 0.32 mm).

There was a large variation in the registration accuracy of different parameter sets ranging from 0.29 mm to 2.5 mm in median registration error and 3.71 mm to 8.9 mm in 95 percentile of the registration error. Three of the parameter sets with the highest registration accuracies are listed in Table 3. Set1 was the parameter set that resulted in the smallest 95 percentile of registration error and, Set2 and Set3 were the parameter sets that provided the smallest median registration error. Gubern-Mérida et al. [26] had also provided a set of parameters for registration of breast DCE-MRI with Elastix. The results of using their parameter set in our simulation study are also reported in Table 3.

The three best parameter sets were applied to the MRI data of the 13 patients as well and registration error was calculated. We also applied the parameter set in Gubern-Mérida et al. [26] to the patient datasets for comparison. The median and inter-quartile ranges of registration errors for the three best parameter sets and the Gubern-Mérida et al. [26] parameters are reported in Table 4. The large registration errors using this parameter set (both in simulation and in patients) highlight the importance of determining the optimal parameter set for the current application.

## Discussions and Conclusions

Registration is required for comparing MRI scans of several visits of a patient to assist the radiologist in accurately detecting a lesion and diagnosing its type. Breast tissue is highly deformable with little rigid landmarks which makes it challenging to align the images of multiple scans and thus non-rigid registration algorithms have to be employed. In general, registration of breast images is very challenging even for motion correction within a single scan [27]. There exist several registration toolkits for non-rigid registration and in this work, we focused on the Elastix toolkit which was capable of registering two breast MRI volumes with high accuracy and in a short time. The highest required accuracy in co-registration depends on the clinical application. Leach et al. [2] reported that average size of invasive tumors - detected in a screening study performed on 649 women with MRI - was 15 mm with the smallest tumor being 5 mm in diameter. Jang et al. [28] in prospectively reviewed more than 11,000 lesions over a 10-year period and reported that average change in the size of

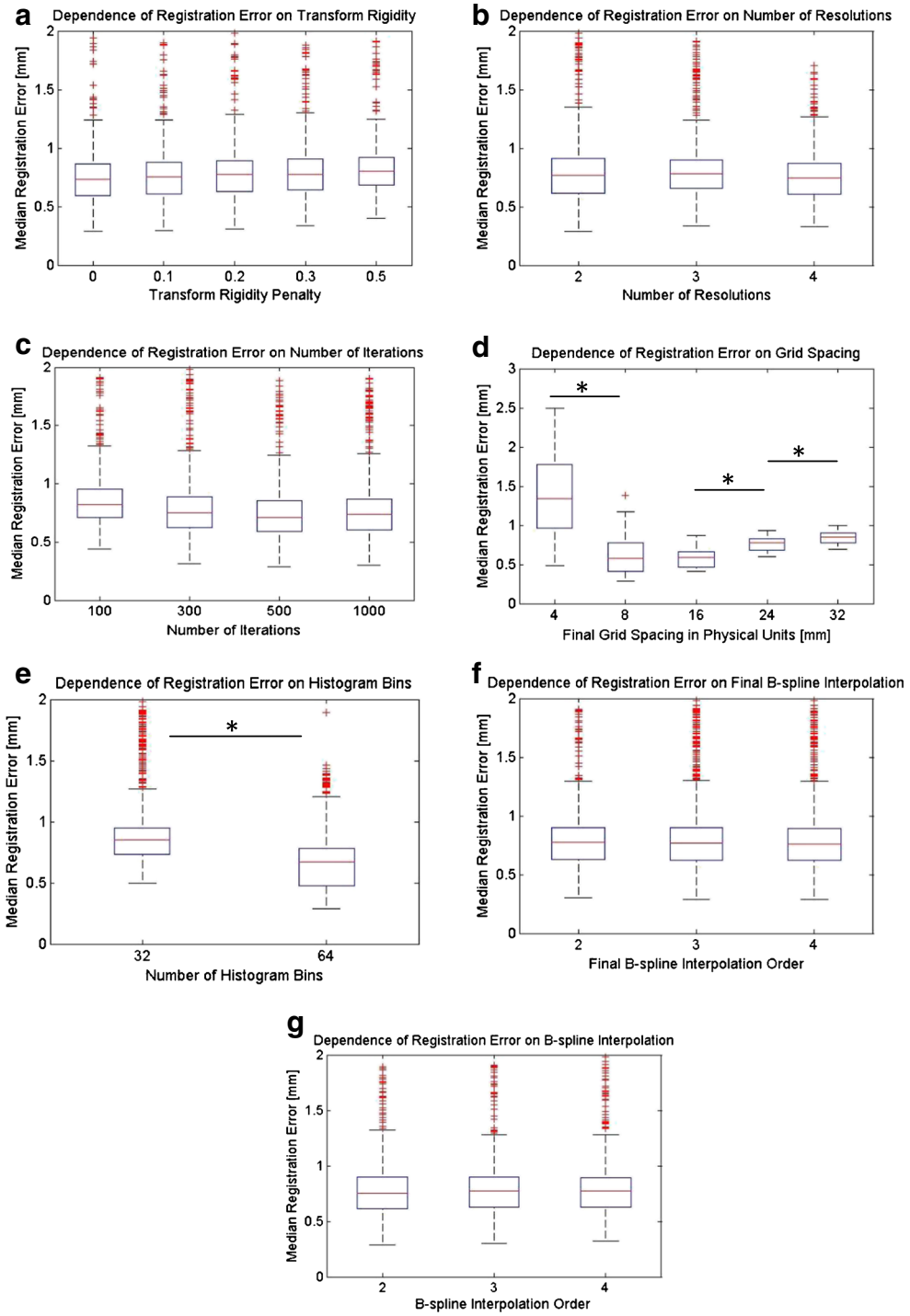


**Fig. 3** Distribution of the median registration error as a function of each parameter. **a** Transform rigidity penalty, **b** number of resolutions, **c** number of iterations, **d** final grid spacing in physical units, **e** number of histogram bins, **f** final B-spline interpolation order, and **g** B-spline interpolation order. The box plots show the median (red line) and interquartile ranges (box) of the distributions for all values of each parameter (red + symbols represent the outliers, and * represnets statistical significance with $p<0.05$)

malignant tumors between multiple visits of patients was 4 mm (0.6 mm per month). These studies demonstrate a registration accuracy of less than 4 mm would be sufficient for clinical applicability of breast registration at multiple visits.

The goal of this study was to propose a framework for determining the optimal parameter set for Elastix and using this framework in breast MRI registration. The framework involved performing numerical simulation of the breast MRI deformation, determining the optimal parameter set, and then evaluating the optimal parameter set using the MRI of a cohort of 13 patients. This study was aimed at breast cancer screening applications with MRI where in most cases there is no tumor. Thus, we did not focus on the large variations that might exist in tumor size between scans or the effects of having a large tumor on registration accuracy. Instead, we studied the registration accuracy for normal breast tissues.

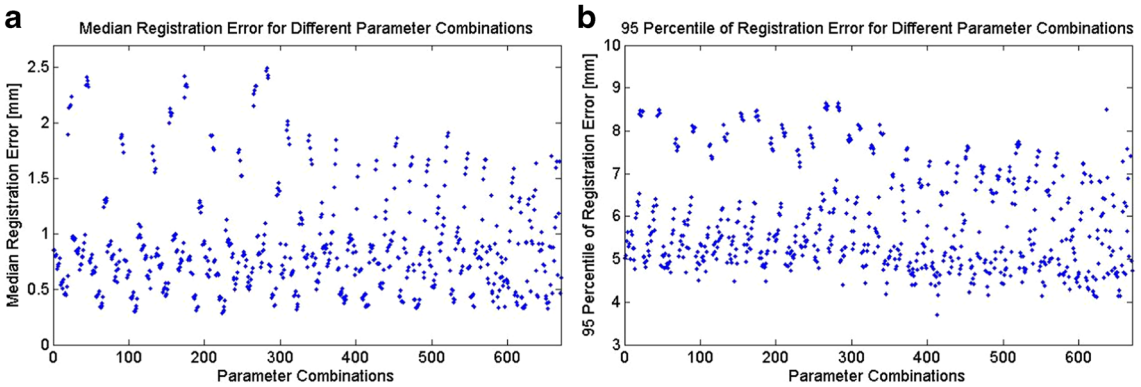


**Fig. 4** **a** Median and **b** 95 percentile of registration error for different combinations of the registration parameters (since there were a large number of parameter combinations, a subset of these combinations is plotted here, in which the sets with less than 0.01 mm difference in median error were shown with one point)

A finite element analysis (FEA)-based simulation was performed to determine the optimal parameter set for registration. The FEA approach provided a realistic deformation of the breast as it relied on the mechanical properties of the breast tissues and deformed the tissues according to the deformations that were applied to the surface of the breast. Such deformation was independent of the B-spline registration in Elastix which used the signal intensity in MRI images to deform and co-register the two volumes.

Mutual information was used as the similarity metric and several parameters of the registration were examined. Statistical analysis (with the non-parametric Wilcoxon rank-sum test) of the registration accuracy obtained by changing individual parameters (as shown in Fig. 3) demonstrated that the registration was not highly sensitive to individual parameters. In most cases, there was not a statistically significant difference between the registration error distributions when only a single parameter was changing (except for grid spacing and number of histogram bins, Fig. 3d, e). However, as shown in Fig. 4, when the entire parameter set was considered, there were large variations between registration errors. Thus, an exhaustive search on various combinations of the parameters was needed to determine the optimal parameter set. This study demonstrated that using the optimal registration parameter set, we were able to obtain a median registration error of approximately 0.3 mm and interquartile ranges of approximately [0.1 1.1] (in mm) in the numerical study.

In order to evaluate the performance of the optimal parameter set (determined in the simulation study), MRI images of a cohort of 13 patients were used. There has been limited work on assessing the registration error in determining landmark locations at different visits. Boehler et al. [12] used expert-labeled landmarks and measured a registration error of 11.7 mm. In this study, the registration was performed on the pre-contrast MRI volumes and its accuracy was evaluated by matching a relatively large number of landmarks that were identified by an expert radiologist in the two visits of the patients.

**Table 3** Optimal parameter combinations for deformable registration with Elastix (determined by the simulation study) and their registration accuracy in numerical simulation study

| Parameter set<br>Parameter | Set1 | Set2 | Set3 | Gubern-Mérida [26] |
|---|---|---|---|---|
| Number of resolutions | 3 | 2 | 2 | 3 |
| Number of iterations | 500 | 500 | 500 | 500 |
| Transform rigidity penalty | 0 | 0 | 0.1 | 0.3 |
| Number of histogram bins | 64 | 64 | 64 | 32 |
| Final grid spacing in physical units | 8 | 8 | 8 | 40 |
| B-spline interpolation order | 3 | 2 | 3 | 1 |
| Final B-spline interpolation order | 2 | 4 | 3 | 1 |
| Registration results | | | | |
| Median [mm] | 0.32 [0.13 1.13] | 0.29 [0.11 1.02] | 0.30 [0.12 1.04] | 1.02 [0.37 2.30] |
| 95 percentile [mm] | 3.71 | 5.02 | 4.70 | 5.48 |
| Run duration [s] | 380 | 330 | 336 | 383 |

**Table 4** Registration error for using the optimal parameter sets in co-registering MRI of the 13 patients, as well as the registration error for parameter set proposed by Gubern-Mérida et al. [26]

| Error metric<br>Parameter set | Median [mm] | 25 percentile [mm] | 75 percentile [mm] |
|---|---|---|---|
| Set1 | 3.4 | 1.8 | 6.8 |
| Set2 | 3.7 | 1.9 | 8.5 |
| Set3 | 3.6 | 1.8 | 8.7 |
| Gubern-Mérida [26] | 4.8 | 2.5 | 8.1 |

A total of 113 pairs of landmarks (~ 11 landmarks per patient) were identified. As reported in Table 4 using the optimal parameter set, we obtained a median registration error of 3.4 mm to 3.7 mm. This table lists three parameter sets that provided the highest registration accuracy. Registration was also performed using the parameter set recommended by Gubern-Mérida et al. [26], in order to assess whether the optimal parameter set was providing more accurate registration results. As reported in Tables 3 and 4, there was a larger registration error (1.02 mm [0.37 mm, 2.30 mm] for the numerical study and 4.8 mm [2.5 mm, 8.1 mm] for the patient study) using this parameter set as compared to the optimal parameter sets. It should be noted that the parameter set in Gubern-Mérida et al. [26] was proposed for motion correction in breast DCE-MRI between different time points of the sequence. Thus, it was not optimized for large deformations that take place between multiple visits of a patient and works well when the deformations are small. This highlights the importance of determining the optimal registration parameter set for the application under investigation.

The duration of the registration process was also evaluated and as expected, increasing the number of resolutions and increasing the number of iterations increased the duration of registration. However, we did not observe any advantage in increasing the number of iterations beyond 500 and there were several parameter sets with 2 resolution levels that provided high registration accuracies.

It is important to note that although the registration accuracy in general increases by increasing the number of resolutions or increasing the number of histogram bins and decreasing the grid spacing, these parameter values make the registration more sensitive to local and smaller structures and thus more sensitive to noise. Thus, in order to have a robust and accurate registration, it is better to use the smallest number of resolutions and histogram bins and the largest grid spacing that provides an accurate registration result. Our results demonstrated that increasing the number of resolution to beyond 3 levels decreased the final registration accuracy (both in numerical and patient studies). Also, decreasing the grid spacing down to 8 mm increased the registration accuracy; however, lowering this parameter to 4 mm significantly increased the error.

Another important difference between the hereby investigated problem (co-registration between multiple visits) versus previously investigated co-registration of DCE-MRI frames of the same visit [16, 17, 26] is the value of "Transform Rigidity Penalty." In DCE-MRI studies, "Transform Rigidity Penalty" was relatively large (0.3) as the breast tissue does not deform significantly during one scan whereas in multiple visits (i.e., large deformation of the breast), the penalty needed to be significantly lower (0 or 0.1) to yield accurate registration.

The level of compression was not fixed between patients or between visits of a patient. It is possible that large compressions applied to the breast could cause internal features to be merged and this may lead to an increase in the registration error. In general, however, large compressions are only applied to the breast during MRI-guided biopsy procedures and not in screening exams.

The current study was performed on breast MRI acquired at a low magnetic field strength of 1.5 T, while most centers nowadays operate with 3 T scanners. The main difference between MRI data acquired at 3 T versus 1.5 T is that the signal-to-noise ratio (SNR) is higher; however, the main parameters probed in this study were related to the imaging resolution (both in-place and through slice) and signal intensity, i.e., the grid spacing, interpolation orders, number if histogram bins, etc. If the resolution is unchanged between 1.5 T and 3 T imaging, then the optimum registration parameters should also remain unchanged.

The main limitation of the proposed pipeline is that the optimal registration parameters are specific to the problem being addressed and cannot be generalized to other problems. However, for any new registration problem, the steps outlined in the pipeline can be repeated to obtain the optimal registration setting.

We will upload our findings including the optimal Elastix parameter set for breast MRI registration to the Elastix wiki website (http://elastix.bigr.nl/wiki/index.php/Parameter_file_database) for other groups to use and evaluate further.

**Acknowledgements** The authors would like to thank the Canadian Institute of Health Research (CIHR) for funding this work through CIHR grant number 115161.

## References

1. Hylton N: Dynamic contrast-enhanced magnetic resonance imaging as an imaging biomarker. J Clin Oncol 24(20):3293–3298, 2006
2. Leach MO: Screening with magnetic resonance imaging and mammography of a UK population at high familial risk of breast cancer: A prospective multicentre cohort study (MARIBS). Lancet 365(9473):1769–1778, 2005
3. Kuhl CK: MRI of breast tumors. Eur. Radiol. 10(1):46–58, 2000
4. Behrens S et al.: Computer assistance for MR based diagnosis of breast cancer: Present and future challenges. Comput Med Imaging Graph 31(4–5):236–247, 2007

5. Partridge SC, Stone KM, Strigel RM, DeMartini WB, Peacock S, Lehman CD: Breast DCE-MRI: Influence of post-contrast timing on automated lesion kinetics assessments and discrimination of benign and malignant lesions. Acad. Radiol. 21(9):1195–1203, 2014
6. Partridge SC, DeMartini WB, Kurland BF, Eby PR, White SW, Lehman CD: Differential diagnosis of mammographically and clinically occult breast lesions on diffusion-weighted MRI. J. Magn. Reson. Imaging 31(3):562–570, 2010
7. Schnall MD, Ikeda DM: Lesion diagnosis working group report. J. Magn. Reson. Imaging 10(6):982–990, 1999
8. David EA, Marshall MB: Review of chest wall tumors: A diagnostic, therapeutic, and reconstructive challenge. Semin. Plast. Surg. 25(1):16–24, 2011
9. Abramovici G, Mainiero MB: Screening breast MR imaging: Comparison of interpretation of baseline and annual follow-up studies. Radiology 259(1):85–91, 2011
10. Frankel SD, Sickles EA, Curpen BN, Sollitto RA, Ominsky SH, Galvin HB: Initial versus subsequent screening mammography: Comparison of findings and their prognostic significance. AJR Am J Roentgenol 164(5):1107–1109, 1995
11. Liberman L, Menell JH: Breast imaging reporting and data system (BI-RADS). Radiol. Clin. North Am. 40(3):409–430, 2002
12. Boehler T, Schilling K, Bick U, Hahn HK: Deformable image registration of follow-up breast magnetic resonance images BT—Biomedical image registration: 4th International Workshop, WBIR 2010, Lübeck, Germany, July 11–13, 2010. Proceedings. In: Fischer B, Dawant BM, Lorenz C Eds. Springer Berlin Heidelberg, Berlin, Heidelberg, 2010, pp 13–24
13. Oliveira FPM, Tavares JMRS: Medical image registration: A review. In: Computer Methods in Biomechanics and Biomedical Engineering, vol. 17, no. 2. Taylor & Francis, 2014, pp 73–93
14. Viergever MA, Maintz JBA, Klein S, Murphy K, Staring M, Pluim JPW: A survey of medical image registration—Under review. Med. Image Anal. 33:140–144, 2016
15. Froh MS, Barber DC, Brock KK, Plewes DB, Martel AL: Piecewise-quadrilateral registration by optical flow—Applications in contrast-enhanced MR imaging of the breast BT—Medical image computing and computer-assisted intervention—MICCAI 2006: 9th International Conference, Copenhagen, Denmark, October 1-. In: Larsen R, Nielsen M, Sporring J Eds. Berlin, Heidelberg: Springer Berlin Heidelberg, 2006, pp 686–693
16. Schnabel JA et al.: Validation of nonrigid image registration using finite-element methods: Application to breast MR images. IEEE Trans Med Imaging 22(2):238–247, 2003
17. Tanner C et al.: Quantitative evaluation of free-form deformation registration for dynamic contrast-enhanced MR mammography. Med. Phys. 34(4):1221, 2007
18. Klein S, Staring M, Murphy K, Viergever MA, Pluim JPW: Elastix: A toolbox for intensity-based medical image registration. IEEE Trans. Med. Imaging 29(1):196–205, 2010
19. Avants BB, Tustison NJ, Song G, Cook PA, Klein A, Gee JC: A reproducible evaluation of ANTs similarity metric performance in brain image registration. Neuroimage 54(3):2033–2044, 2011
20. Mehrabian H, Campbell G, Samani A: A constrained reconstruction technique of hyperelasticity parameters for breast cancer assessment. Phys. Med. Biol. 55(24):7489–7508, 2010
21. Mehrabian H, Samani A: An iterative hyperelastic parameters reconstruction for breast cancer assessment. In: Proceedings of SPIE Medical Imaging: Physiology, Function, and Structure from Medical Images, 2008, vol. 6916, pp 69161C–69161C–9
22. Samani A, Zubovits J, Plewes D: Elastic moduli of normal and pathological human breast tissues: An inversion-technique-based investigation of 169 samples. Phys Med Biol 52:1565–1576, 2007
23. Xu H, Varghese T, Madsen EL: Analysis of shear strain imaging for classifying breast masses: Finite element and phantom results. Med. Phys. 38(11):6119–6127, 2011
24. Rueckert D, Sonoda LI, Hayes C, Hill DL, Leach MO, Hawkes DJ: Nonrigid registration using free-form deformations: Application to breast MR images. IEEE Trans Med Imaging 18(8):712–721, 1999
25. Pluim JPW, Maintz JBA, Viergever MA: Mutual-information-based registration of medical images: A survey. IEEE Trans Med Imaging 22(8):986–1004, 2003
26. Gubern-Mérida A et al.: Automated localization of breast cancer in DCE-MRI. Med. Image Anal. 20(1):265–274, 2015
27. Ojeda-Fournier H, Choe KA, Mahoney MC: Recognizing and interpreting artifacts and pitfalls in MR imaging of the breast. Radiographics 27 Suppl 1:S147–S164, 2007
28. Jang JY et al.: Clinical significance of interval changes in breast lesions initially categorized as probably benign on breast ultrasound. Medicine (Baltimore). 96(12):1–7, 2017